Geometrical Structures and Fundamental Characteristics of Microwave Stepped-Impedance Resonators

Morikazu Sagawa, *Member, IEEE*, Mitsuo Makimoto, *Member, IEEE*, and Sadahiko Yamashita, *Member, IEEE*

***Abstract*—$\lambda_g/4$-, $\lambda_g/2$-, and λ_g-type transmission-line stepped-impedance resonators (SIR's) have been proposed and various practical applications have been reported on the basis of the analysis related to each resonator. This paper standardizes these three types of SIR's and systematically summarizes their fundamental characteristics, such as resonance conditions, resonator length, spurious (higher order) responses, and equivalent circuits. Practical applications which employ features of three types of SIR's are investigated with demonstrations of specific structures. Original design formulas with respect to λ_g-type dual-mode resonators are analytically derived. Advanced SIR's using composite material and multisteps are also introduced and their availability is discussed.**

***Index Terms*—Fundamental characteristics, practical applications, microwave resonators.**

I. Introduction

TRANSMISSION lines with stepped-impedance resonators (SIR's) have been frequently used as resonators [1] for analyzing discontinuity in a transmission line with an impedance step. However, SIR's had rarely been employed until the design formulas of $\lambda_g/4$-type coaxial SIR's were analytically derived and applied to bandpass filters [2] and antenna duplexers [3] for mobile communication equipment. Research and development has mainly progressed in the coaxial resonators [4]–[6]. Recently, the concept of SIR's has been advanced to half- and one-wavelength [7], [8] resonators with a microstrip structure, and then various applications using their structural features have been reported. However, the investigation of SIR's was based on the individual analysis.

This paper standardizes $\lambda_g/4$-, $\lambda_g/2$-, and λ_g-type SIR's and systematically summarizes fundamental characteristics of these three types of SIR's. Practical examples employing structural features of the three types of SIR's are demonstrated and their availability is discussed. Original design formulas of λ_g dual-mode resonators, both two- and four-port devices, are analytically derived. Two resonators enlarging the SIR concept employing composite material and multisteps are also introduced and their usefulness and shortcomings are discussed.

Manuscript received October 10, 1996; revised March 24, 1997.

The authors are with Matsushita Research Institute Tokyo, Inc., Tama-ku Kawasaki 214, Japan.

Publisher Item Identifier S 0018-9480(97)04458-X.

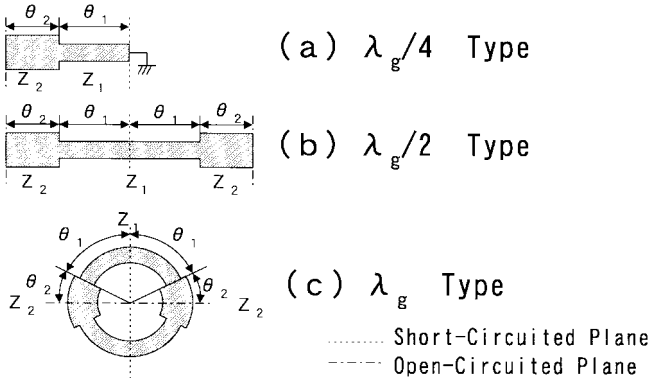

Fig. 1. Basic structure of SIR.

II. Basic Structures of the SIR's and their Characteristics

Basic structures of SIR's and their characteristics are systematically summarized in this section.

A. Resonance Properties of the SIR's

Fig. 1 shows basic structures of the three types of SIR's. The $\lambda_g/2$ type shown in Fig. 1(b) has a structure in which both ends are open; however, a structure in which both ends are short also exists. Transmission lines between open and short planes have different characteristic impedances Z_1 and Z_2 and corresponding lengths θ_1 and θ_2. The fundamental structural element common to all three types of SIR's is a composite transmission line with both open and short planes involving a step junction. $\lambda_g/4$-, $\lambda_g/2$-, and λ_g-type SIR's are composed of one, two, and four fundamental elements, respectively. In all types of SIR's, resonance conditions [2], [4], [7] can be derived from the structural fundamental element. Ignoring the influences of a step discontinuity, the admittance of the composite transmission line from the open plane Y_i is given as follows:

$$Y_i = jY_2 \frac{Y_2 \tan\theta_1 \cdot \tan\theta_2 - Y_1}{Y_2 \tan\theta_1 + Y_1 \tan\theta_2}. \tag{1}$$

The resonance condition from $Y_i = 0$ can be described as follows:

$$\tan\theta_1 \cdot \tan\theta_2 = R_Z \tag{2}$$

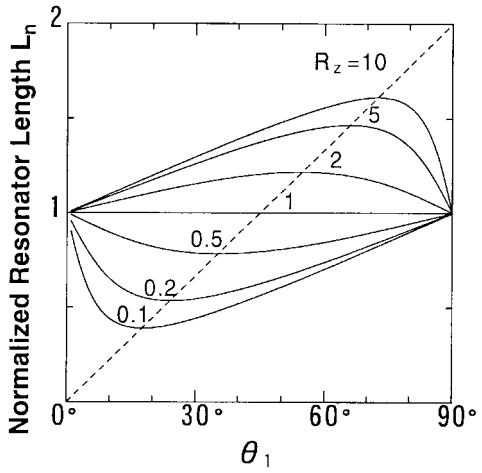

Fig. 2. Resonance conditions of SIR.

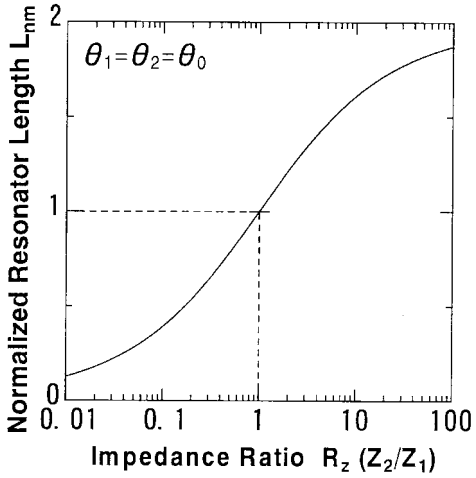

Fig. 3. Relationship between impedance ratio and normalized resonator length.

where impedance ratio is

$$R_Z = Y_1/Y_2 = Z_2/Z_1.$$

Resonance conditions in the case of ordinary uniform impedance resonators (UIR's) can be determined based solely on the length of lines; however, in determining resonance conditions of SIR's, both the length and the impedance ratio must be taken into account. Therefore, SIR's have more design parameters than UIR's, and impedance ratio R_Z is an important parameter in investigating SIR's. The lengths of the three types of SIR's are represented by θ_{TA}, θ_{TB}, and θ_{TC}, respectively,

$$\begin{aligned}\theta_{TA} &= \theta_1 + \theta_2 \\ &= \theta_1 + \tan^{-1}\left(\frac{R_Z}{\tan\theta_1}\right) \\ &= \theta_{TB}/2 = \theta_{TC}/4. \end{aligned} \tag{3}$$

Fig. 2 shows the relationship between the length θ_1 and the resonator length L_n. The resonator length L_n is the normalized resonator length of the three types of SIR's with respect to the length of corresponding UIR's $\pi/2$, π, and 2π, respectively,

$$L_n = \theta_{TA}/(\pi/2) = \theta_{TB}/\pi = \theta_{TC}/(2\pi). \tag{4}$$

Fig. 2 clearly shows that the resonator length attains its maximum value when $R_Z \geq 1$ and its minimum value when $R_Z \leq 1$. The condition yielding a maximum and a minimum length [2], [4] is as follows:

$$\theta_1 = \theta_2 \equiv \theta_0 = \tan^{-1}\sqrt{R_Z}. \tag{5}$$

When $R_Z = 1$, the resonator length is constant because the resonator is a UIR. Fig. 3 shows the relationship between impedance ratio R_Z and normalized resonator length L_{nm} when $\theta_1 = \theta_2 \equiv \theta_0$. Ignoring the influence of a step discontinuity, the resonator length of a SIR is shown to be less than twice that of the corresponding UIR even if the adopted R_Z is as large as possible.

The resonator length and corresponding spurious (higher order) frequencies can be adjusted by changing the impedance ratio R_Z [4], [7]. When $\theta_1 = \theta_2 \equiv \theta_0$, the fundamental resonance frequency is represented as f_0 and the lowest spurious frequency of $\lambda_g/4$-, $\lambda_g/2$-, and λ_g-type SIR's are represented as f_{SA}, f_{SB}, and f_{SC}, respectively. The relationship between fundamental and spurious frequencies [4], [7] is given by

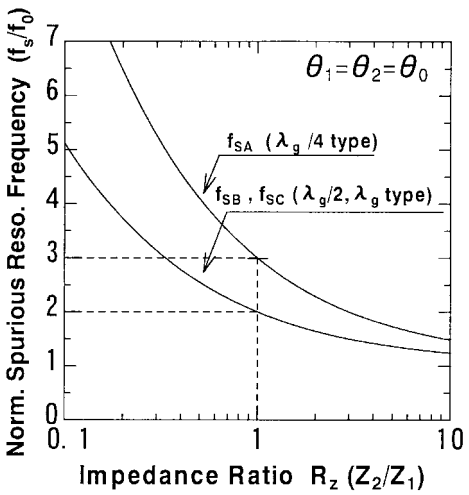

Fig. 4. Relationship between impedance ratio and normalized spurious resonance frequency.

$$\frac{f_{SA}}{f_0} = \frac{\pi}{\tan^{-1}\sqrt{R_Z}} - 1 \tag{6}$$

$$\frac{f_{SB}}{f_0} = \frac{f_{SC}}{f_0} = \frac{\pi}{2\tan^{-1}\sqrt{R_Z}}. \tag{7}$$

Fig. 4 shows the results of the above relationships. Making the resonator length as short as possible is useful for enlarging the span between fundamental and spurious frequencies. Reducing R_Z is indispensable for miniaturizing the resonator length. The above discussion assumes the TEM mode and ignores a step discontinuity; therefore, three-dimensional (3-D) electromagnetic (EM) analysis is necessary to rigorously solve the resonance frequency.

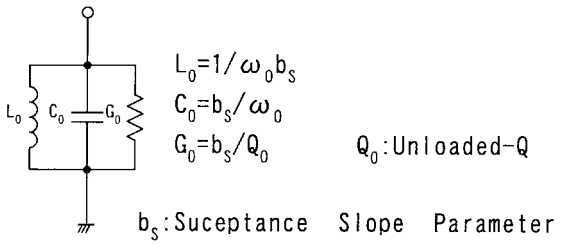

Fig. 5. An equivalent circuit of SIR.

B. Susceptance Slope Parameters

In designing bandpass filters using distributed resonators, lumped-element description rather than direct analysis of distributed circuits is often suitable. A distributed SIR in the resonating state can be expressed as a lumped-element parallel-resonance circuit [4] consisting of L_0, C_0, and G_0 as shown in Fig. 5.

The susceptance slope parameter b_S can be obtained from its definition as follows:

$$b_S = \frac{\omega}{2}\frac{dB_S}{d\omega}\bigg|_{\omega=\omega_0}$$

where ω_0 is the angular resonance frequency and $B_S(\omega)$ is the susceptance from the open ended portion of a SIR. Element values shown as L_0, C_0, and G_0 are given as follows:

$$L_0 = \frac{1}{\omega_0 b_S}, \qquad C_0 = \frac{b_S}{\omega_0}, \qquad G_0 = \frac{b_S}{Q_0} \tag{8}$$

where Q_0 is the unloaded $-Q$ of a SIR. In the case of $\theta_1 = \theta_2 \equiv \theta_0$, the susceptance slope parameters of $\lambda_g/4$-, $\lambda_g/2$-, and λ_g-type SIR's are expressed as b_{SA0}, b_{SB0}, and b_{SC0}, respectively. b_{SA0}, b_{SB0}, and b_{SC0} are obtained as follows:

$$b_{\mathrm{SA0}} = \theta_0 Y_2 = \frac{\tan^{-1}\sqrt{R_Z}}{Z_2}$$
$$b_{\mathrm{SB0}} = 2\theta_0 Y_2 = \frac{2\tan^{-1}\sqrt{R_Z}}{Z_2}$$
$$b_{\mathrm{SC0}} = 4\theta_0 Y_2 = \frac{4\tan^{-1}\sqrt{R_Z}}{Z_2}. \tag{9}$$

Therefore, element values shown in (8) can be calculated using the above susceptance slope parameters and unloaded $-Q$, calculated independently.

Based on the above discussion, fundamental characteristics can be systematically derived by introducing the concept of a composite transmission line with a step junction.

III. Practical Resonator Structures and Their Applications

In this section, practical resonator structures and useful applications of the three types of SIR's are demonstrated.

A. $\lambda_g/4$-Type SIR's

Application of SIR's to bandpass filters and antenna duplexers for mobile communications have been investigated due to excellent electrical performances of SIR's such as a shorter resonator length less than quarter-wavelength and harmonics suppression characteristics. Coaxial SIR's using high dielectric-constant material, as shown in Fig. 6, have been put into practical use [5], [6]. Fig. 6(a) shows the preferable structure for minimizing R_Z. It consists of a rectangular outer conductor and a round and rectangular inner conductor for high impedance of a short-ended portion and low impedance of an open-ended portion. $R_Z = 0.1(Z_1 = 10\ \Omega, Z_2 = 1\ \Omega)$ is realized in the material of $\varepsilon_r = 95$. The resonator length can be reduced to less than 40% of a UIR made of the same material. Fig. 6(b) has a double coaxial structure for improvement of useless open-ended portions of a SIR. By adopting this structure, the resonator length can be easily reduced to less than 30% of a UIR with little degradation of unloaded Q. In the 400-MHz band, the resonator length of about 6 mm has been reported [6] using the dielectric material of $\varepsilon_r = 95$.

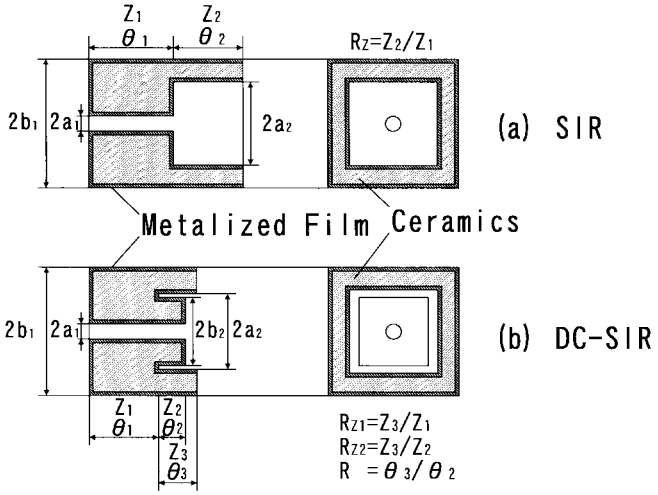

Fig. 6. Some structures of miniaturized coaxial SIR's.

The unloaded-Q is one of the significant parameters to determine the resonator structure. The unloaded-Q of SIR's shown in Fig. 6 mainly depends on the conductor losses in the case of low-loss dielectric material. The Q based on the conductor losses, Q_C, depends on the structure of the resonators and can be obtained by calculating the stored energy and conductor losses. On the assumption of the TEM mode, Q_C values of SIR's [5], [6] (shown in (10) and (11) at the bottom of the following page) corresponding to Fig. 6 can be calculated, where

- $\mathbf{H}$ vector of the magnetic field;
- $\mathbf{H_t}$ tangent component of the magnetic field;
- δ shin depth;
- μ permeability of the material;
- ε_r relative dielectric constant of the material;
- λ_0 wavelength in free space;
- C_i $(i = 1,2,3)$ capacitance per unit length of the line i;
- Z_i $(i = 1,2,3)$ characteristic impedance of the line i.

However, SIR's shown in Fig. 6 have different resonator lengths. Therefore, the parameter FM is defined by the ratio of the Q_C value and resonator volume. Introducing this

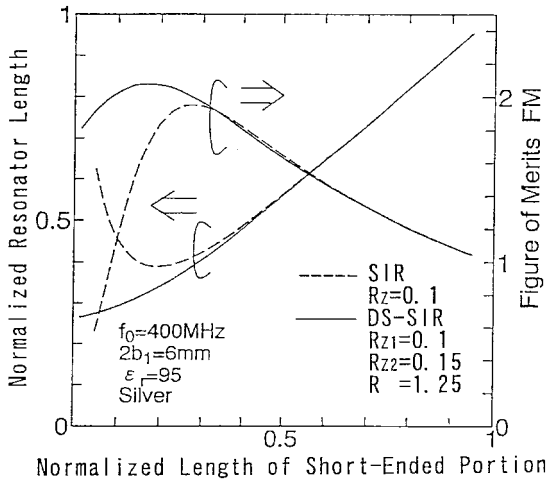

Fig. 7. Figure of merits of SIR and DC-SIR.

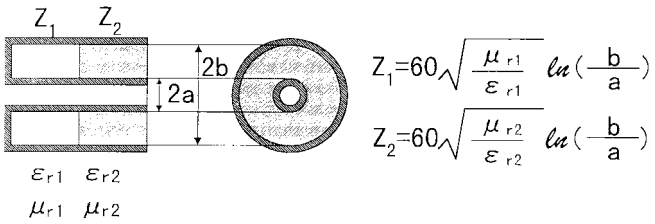

Fig. 8. A structure of SIR using composite material.

parameter, various resonators with different volume can be reasonably estimated. Fig. 7 shows the comparison between SIR's and double-coaxial SIR's (DC-SIR's) of the same size with an inner and an outer conductor. Fig. 7 makes it clear that the DC-SIR has excellent figure of merits in the condition of a shorter resonator length than the SIR. However, a complicated manufacturing process is necessary to make DC-SIR's, they are suitable as the resonator of lower than 1 GHz, i.e., 400-MHz band.

$\lambda_g/4$-type SIR's using high dielectric-constant material have been in popular use because of their compactness. To maximize the unloaded $-Q$ of a coaxial resonator, the diameter ratio of inner and outer conductors should be selected 3.7. SIR's using composite material shown in Fig. 8, which are expected to be more compact and to yield higher values of Q. ε_{r1} and ε_{r2} indicate relative dielectric constants and μ_{r1} and μ_{r2} indicate relative permeability.

The characteristic impedance is given by

$$60\sqrt{\frac{\mu_r}{\varepsilon_r}}\ln\left(\frac{b}{a}\right).$$

The impedance ratio R_Z can be obtained as

$$R_Z = \frac{Z_2}{Z_1} = \sqrt{\frac{\mu_{r2}}{\mu_{r1}}}\sqrt{\frac{\varepsilon_{r1}}{\varepsilon_{r2}}}. \tag{12}$$

A wavelength reduction factor is given by $1/\sqrt{\mu_r\varepsilon_r}$, therefore, both $\mu_{r1} > \mu_{r2}$, $\varepsilon_{r1} < \varepsilon_{r2}$ and μ_r, ε_r as large as possible are indispensable for miniaturization. Finding magnetic material having large μ_r and excellent HF characteristics is very difficult. One reported example [9] uses air for Z_1 and high dielectric material for Z_2, which is the condition of $\mu_{r1} = \mu_{r2} = 1$, $\varepsilon_{r1}(=1) \ll \varepsilon_{r2}$. Sufficient reduction factor cannot be obtained when air is used as the dielectric material of a short-ended portion. However, applying this structure for use in the VHF band is appropriate because small- and partial-sized dielectric material is used.

Bandpass filters with steeper attenuation poles [10], [11] are another mentioned application using the characteristics of SIR's. In the coaxial or stripline structure shown in Fig. 9, main coupling is attained by electric coupling at open-ended portions, and sub-coupling is attained by magnetic coupling at short-ended portions. The existence of sub-coupling generates attenuation poles in the stopband of bandpass filters. The frequencies of attenuation poles can be controlled by adjusting the sub-coupling factor. The degree of sub-coupling can be controlled independently from the degree of main coupling. Not only the two-stage resonator structure shown in Fig. 9, but also multistage structures, can be expected to yield elliptic function filters.

$$Q_C = \frac{2}{\delta}\frac{\iiint |\mathbf{H}|^2\,dV}{\iint |\mathbf{H_t}|^2\,dS} = \frac{2b_1}{\delta\mu}Q_C(j) \quad (j = \text{SIR, DC-SIR})$$

$$Q_C(\text{SIR}) = \frac{A_1C_1Z_1^2 + A_2B_2C_2Z_2^2}{\frac{A_1}{8}\left(1+\frac{4b_1}{\pi a_1}\right) + \frac{A_2B_2}{8}\left(1+\frac{b_1}{a_2}\right) + \frac{4b_1\sqrt{\varepsilon_r}}{\lambda_0}\left\{\ln\left(\frac{4b_1}{\pi a_1}\right) + B_1\ln\left(\frac{4a_2}{\pi a_1}\right)\right\}}$$

$$A_1 = 2\theta_1 + \sin 2\theta_1,\ A_2 = 2\theta_2 - \sin 2\theta_2,$$

$$B_1 = \cos^2\theta_1, \qquad B_2 = \frac{\cos^2\theta_1}{\sin^2\theta_2}. \tag{10}$$

$$Q_C(\text{DC-SIR}) = \frac{A_1C_1Z_1^2 + A_2B_2C_2Z_2^2 + A_3B_3C_3Z_3^2}{\frac{A_1}{8}\left(1+\frac{4b_1}{\pi a_1}\right) + \frac{A_2B_2}{8}\left(\frac{4b_1}{\pi a_1}+\frac{b_1}{b_2}\right) + \frac{A_3B_3}{8}\left(1+\frac{b_1}{a_2}\right) + \frac{4b_1\sqrt{\varepsilon_r}}{\lambda_0}\left\{\ln\left(\frac{4b_1}{\pi a_1}\right) + B_1\ln\left(\frac{a_2}{b_2}\right) + B_2\ln\left(\frac{4b_2}{\pi a_1}\right)\right\}}$$

$$A_1 = 2\theta_1 + \sin 2\theta_1,\ A_2 = 2\theta_2 + \sin 2\theta_2,\ A_3 = 2\theta_3 - \sin 2\theta_3,$$

$$B_1 = \cos^2\theta_1, \qquad B_2 = \frac{\cos^2\theta_1}{\cos^2\theta_2}, \qquad B_3 = \frac{\cos^2\theta_1}{\sin^2\theta_3}. \tag{11}$$

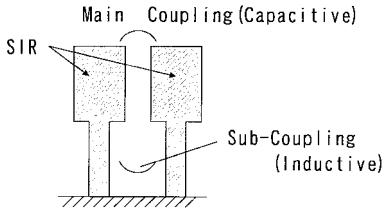

Fig. 9. Interstage coupling of $\lambda_g/4$-type SIR.

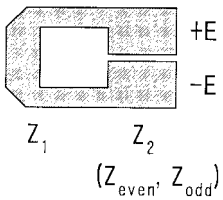

Fig. 10. Structure of split-ring SIR.

B. $\lambda_g/2$-Type SIR's

There are two $\lambda_g/2$-type SIR's: one is a resonator with open-ended portions and the other is with short-ended portions. In the stripline structure, an open-ended-type resonator is suitable for no RF short-circuited points. Paying attention to the ability to control spurious responses of SIR's [7], [12], [13] by impedance ratio R_Z, bandpass filters with wide stopband characteristics have been also investigated. From these investigations, generalized design formulas for stripline SIR bandpass filters, which use parallel coupled lines with arbitrary coupling angles, have been derived [7].

For miniaturizing open-ended $\lambda_g/2$-type SIR's, a hairpin-type structure with coupled open-ended portions [14], as shown in Fig. 10, is preferable. In this resonator, the characteristic impedance of open-ended portions can be considered to be an odd-mode impedance of coupled lines, lower than the characteristic impedance of single transmission lines, and the impedance ratio R_Z can be smaller. This structure is the combination of split-ring resonators [15], [16], which are composed of a ring-shaped line and a connecting capacitor, and SIR's. This is the most useful structure of $\lambda_g/2$-type SIR's. These types of resonators have been practically applied not only to filters, but also to oscillators [14] and oscipliers [17].

Fig. 11 shows examples of balanced mixers which use split-ring SIR's. Balanced mixers can be easily made by combining both functions of a balance–unbalance transformer and an opposite phase of open-ended portions within split-ring resonators.

The SIR's with two different impedance transmission lines have been advanced to multistepped open-ended $\lambda_g/2$-type resonators [18] and tapered transmission-line resonators as an ultimate structure, shown in Fig. 12(a) and 12(b), respectively. Multistepped resonators are considered to be useless because they have no distinguishing features as compared with two-step SIR's and tapered resonators. However, multistepped resonators are extremely useful for analyzing tapered resonators, especially linear-tapered resonators [19], which are difficult to directly analyze. Through this analysis method, fundamental characteristics of linear-tapered transmission-line

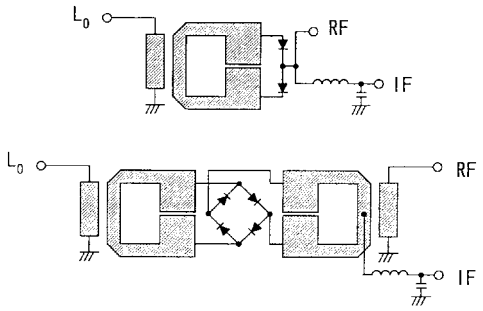

Fig. 11. Some circuit diagrams of balanced mixers.

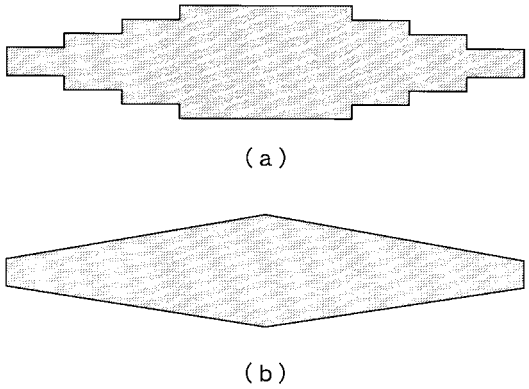

Fig. 12. (a) Multistep $\lambda_g/2$-type SIR and (b) linear-tapered transmission-line resonator.

resonators and their filter-design parameters can be easily derived. Experimental results of fabricated filters based on these results have shown close agreement with the design data [19]. From these results, the design method using multistepped description is verified to be very useful.

The coupling using linear-tapered transmission lines is based on asymmetric coupled transmission lines [20]. It can be obtained stronger than the electric coupling between open-ended portions. Thus, filters with a larger bandwidth can be easily realized through use of linear-tapered transmission-line resonators.

Recently, multilayered composite material with gradient dielectric constant [21] has been investigated for use in microwave devices. Using this material, multistepped and tapered resonators can be easily fabricated. Novel applications of such inhomogeneous media will be expected to extend to microwave devices.

C. λ_g-Type SIR's

λ_g-type resonators are useless as single-mode resonators because of their large structures. Their main applications use two orthogonal modes within one wavelength ring resonator [8], [22], [23] and their applications are useful. These orthogonal modes can be maintained in the case of λ_g-type SIR's. There are two different methods using dual modes within λ_g-type SIR's. One is a four-port device using two independent modes, the other is a two-port device using the coupling between dual modes.

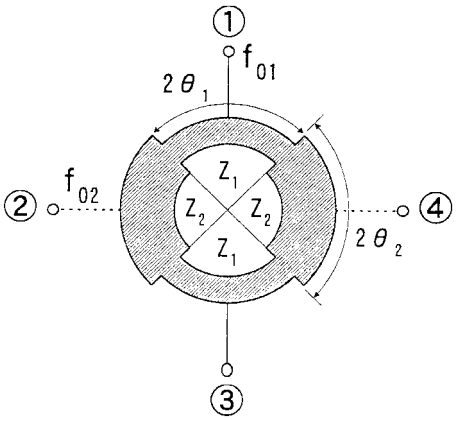

Fig. 13. Structure of SIR with dual resonance frequencies using orthogonal modes.

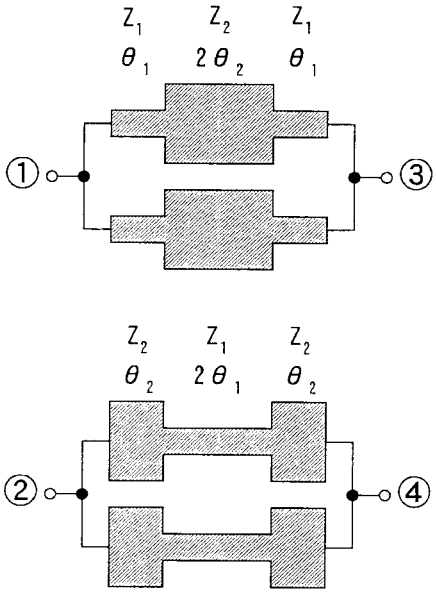

Fig. 14. Equivalent circuits of SIR with dual resonance frequencies.

The first investigated application is a four-port device. Fig. 13 shows the dual-mode SIR, which is composed of transmission lines with impedance ratio R_Z and has two different resonance frequencies f_{01} and f_{02}. By electrically exciting the center of lines having respective impedance Z_1, Z_2, two independent resonance modes shown in Fig. 14 generate each other. These two resonance modes are indicated in the structures which connect parallel open-ended $\lambda_g/2$-type SIR's with different structures. Resonance conditions at $\theta_1 = \theta_2 \equiv \theta_0$ can be obtained as follows:

$$\tan^2\left(\frac{\theta_0 f_{01}}{f_0}\right) = \frac{1}{R_Z}$$
$$\tan^2\left(\frac{\theta_0 f_{02}}{f_0}\right) = R_Z \qquad (13)$$

where

f_0 resonance frequency of λ_g-type UIR's;
f_{01} resonance frequency of λ_g-type SIR's in exciting position 1;

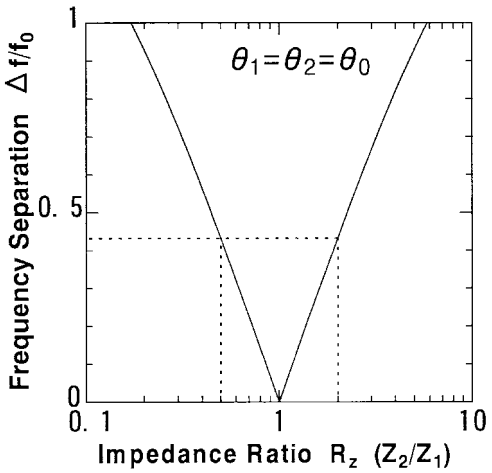

Fig. 15. Resonance frequency separation of SIR with dual resonance frequencies.

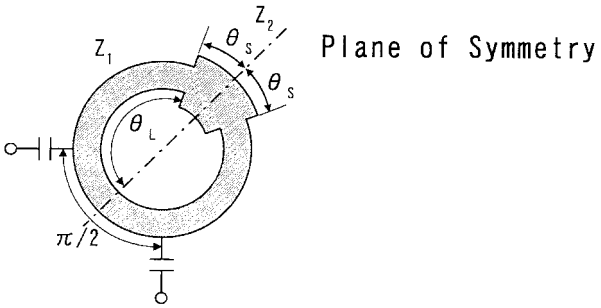

Fig. 16. A structure of dual-mode filters.

f_{02} resonance frequency of λ_g-type SIR's in exciting position 2;
θ_0 one-eighth of the total electrical length of UIR at f_0.

The frequency difference between dual-mode resonance can be normalized by f_0 as follows:

$$\frac{\Delta f}{f_0} = \frac{4}{\pi}\left|\tan^{-1}\sqrt{\frac{1}{R_Z}} - \tan^{-1}\sqrt{R_Z}\right|. \qquad (14)$$

Fig. 15 shows the calculation results of the above relationships. When $R_Z = 0.5$, $\Delta f/f_0 = 0.43$ can be obtained and resonators which act as duplexers can be designed.

The second application is a two-port device. Fig. 16 shows the structure of a two-port dual-mode filter, which uses the coupling between two orthogonal resonance modes. To make a coupling between two orthogonal modes within the resonator, the structure must have the following characteristics [8].

1) Input and output ports are spatially separated 90° from each other.
2) A discontinuity or other means of generating reflected waves against incident waves are introduced at a location that is offset 135° from input and output.
3) The circuit geometry includes a plane of symmetry.

The presence of an impedance step within the resonator yields a dual-mode filter as shown in Fig. 17. An impedance step is used as a perturbation to solve two degenerate modes within one wavelength ring resonators. Various parameters of

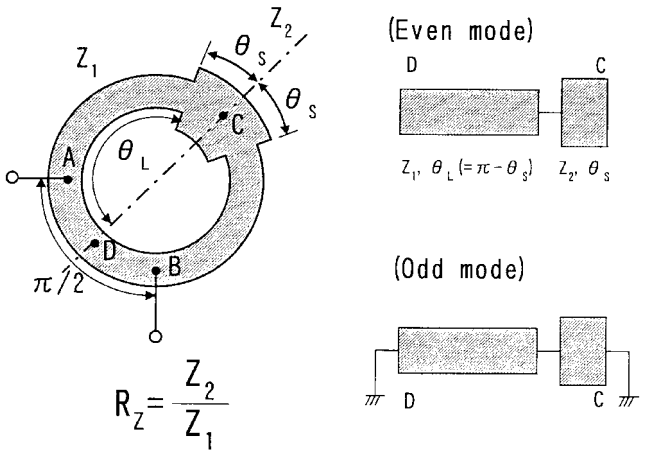

Fig. 17. Equivalent circuits of dual-mode resonators.

an impedance step can be used to control the coupling between two orthogonal modes, as will be described in detail later.

The coupling coefficient between dual-modes corresponds to the eigenvalues of the symmetry circuit in both even- and odd-mode excitation. The coupling coefficient k can be obtained as follows:

$$k = \frac{|f_{\text{even}} - f_{\text{odd}}|}{f_{\text{even}} + f_{\text{odd}}} \tag{15}$$

where f_{even} is the even-mode resonance frequency and f_{odd} is the odd-mode resonance frequency. Even- and odd-modes excitation correspond to the equivalent circuits with open and short at the reference plane, respectively. Two resonance modes within the resonator, which comprises dual-mode filters shown in Fig. 16, can be indicated as even- and odd-modes equivalent circuits shown in Fig. 17. The electrical length of each line is represented by the resonance frequency of uniform impedance ring resonators f_0. f_{even} and f_{odd} are newly derived in this paper as follows:

(Even mode)

$$\tan\left(\frac{\theta_S f_{\text{even}}}{f_0}\right) + R_Z \tan\left(\frac{\theta_L f_{\text{even}}}{f_0}\right) = 0 \tag{16}$$

(Odd mode)

$$R_Z \tan\left(\frac{\theta_S f_{\text{odd}}}{f_0}\right) + \tan\left(\frac{\theta_L f_{\text{odd}}}{f_0}\right) = 0. \tag{17}$$

Considering $\theta_S \ll \theta_L$ in the design of narrow-band filters, (16) and (17) can be modified as follows:

(Even mode)

$$\left(\frac{\theta_S f_{\text{even}}}{f_0}\right) + R_Z\left(\frac{\theta_L f_{\text{even}}}{f_0} - \pi\right) = 0 \tag{18}$$

(Odd mode)

$$R_Z\left(\frac{\theta_S f_{\text{odd}}}{f_0}\right) + \left(\frac{\theta_L f_{\text{odd}}}{f_0} - \pi\right) = 0. \tag{19}$$

Therefore, the coupling coefficient k can be given as follows:

$$k = \frac{\theta_S}{\theta_L}\left|R_Z - \frac{1}{R_Z}\right| = \frac{\theta_S}{\pi}\left|R_Z - \frac{1}{R_Z}\right| \tag{20}$$

because $\theta_L \cong \pi$.

The center frequency f_{center} of a dual-mode resonator with an impedance step, which represents the average of f_{even} and f_{odd}, is given as follows:

$$f_{\text{center}} = \frac{f_{\text{even}} + f_{\text{odd}}}{2} = \frac{\pi f_0}{\theta_L} \cong f_0. \tag{21}$$

There are various coupling methods of two orthogonal modes. When an impedance step is used, the center frequency is nearly constant as shown in (21). Therefore, the correction of a resonator length is unnecessary. An additional advantage of this coupling method is that two different design parameters can be changed: electrical length and impedance ratio of an impedance step.

IV. Conclusion

Fundamental characteristics of $\lambda_g/4$-, $\lambda_g/2$-, and λ_g-types SIR's are systematically summarized. Their excellent features and applications using these features are discussed in detail.

Transmission-line resonators with a simple structure have usually been used in filters and oscillators for easy analysis and accurate design forecast. However, not only fundamental performances such as compactness and high Q value, but also functional characteristics such as spurious suppression and affinity to active devices, have been strongly required. That is, compact resonators with high Q value and high quality performances are earnestly desired.

Recently, popularization of microwave-circuit simulators has been progressing steadily, and high-performance computers have made EM analysis a usable design tool. From these conditions, SIR's and newly developed resonators based on advanced SIR concepts have been practically used in various applications. These include coaxial and stripline structures as well as planar circuits.

References

[1] A. Gopinath, A. F. Thomson, and I. M. Stephenson, "Equivalent circuit parameters of microstrip step change in width and cross junction," *IEEE Trans. Microwave Theory Tech.*, vol. MTT-24, pp. 142–144, Mar. 1976.

[2] M. Makimoto and S. Yamashita, "Compact bandpass filters using stepped impedance resonators," *Proc. IEEE*, vol. 67, pp. 16–19, Jan. 1979.

[3] M. Makimoto, H. Endoh, S. Yamashita, and K. Tanaka, "Compact duplexer for 400-MHz band land mobile radio equipment," in *33rd IEEE Veh. Technol. Conf., Dig.*, Toronto, Ont. Canada, May 1983, pp. 201–204.

[4] M. Sagawa, M. Makimoto, and S. Yamashita, "A design method of bandpass filters using dielectric-filled coaxial resonators," *IEEE Trans. Microwave Theory Tech.*, vol. MTT-33, pp. 152–157, Feb. 1985.

[5] M. Sagawa, M. Makimoto, K. Eguchi, and F. Fukushima, "Miniaturized antenna duplexers for portable radio telephone terminals," *IEICE Trans.*, vol. E74, no. 5, pp. 1221–1225, May 1991.

[6] M. Sagawa, M. Matsuo, M. Makimoto, and K. Eguchi, "Miniaturized stepped impedance resonators with a double coaxial structure and their application to bandpass filters," *IEICE Trans.*, vol. E78-C, no. 8, pp. 1051–1057, Aug. 1995.

[7] M. Makimoto and S. Yamashita, "Bandpass filters using parallel coupled stripline stepped impedance resonators," *IEEE Trans. Microwave Theory Tech.*, vol. MTT-28, pp. 1413–1417, Dec. 1980.

[8] H. Yabuki, M. Sagawa, M. Matsuo, and M. Makimoto, "Stripline dual-mode ring resonators and their application to microwave devices," *IEEE Trans. Microwave Theory Tech.*, vol. 44, pp. 723–729, May 1996.

[9] S. Yamashita and M. Makimoto, "Miniaturized coaxial resonator partially loaded with high-dielectric-constant microwave ceramics," *IEEE Trans. Microwave Theory Tech.*, vol. MTT-31, pp. 697–703, Sept. 1983.

[10] T. Ishizaki and T. Uwano, "A stepped-impedance comb-line filter fabricated by using ceramic lamination technique," in *1994 IEEE MTT-S Int. Microwave Symp. Dig.*, San Diego, CA, May 1994, pp. 617–620.
[11] H. Katoh, H. Matsumoto, and T. Nishikawa, "A miniaturized and high performance dielectric monoblock filter for digital cordless telephone system," in *1994 APMC Dig.*, Tokyo, Japan, pp. 71–74, Dec. 1994.
[12] C. Y. Ho and J. H. Weidman, "Half-wavelength and step impedance resonators aid microstrip filter design," *Microwave Syst. News*, pp. 88–103, Oct. 1983.
[13] Y. Qian, K. Yanagi, and E. Yamashita, "Characterization of a folded stepped-impedance resonator for miniature microstrip bandpass filter applications," in *Proc. 1995 European Microwave Conf.*, Bologna, Italy, Sept. 1995, pp. 1209–1211.
[14] H. Yabuki, H. Endoh, M. Sagawa, and M. Makimoto, "Hairpin-shaped stripline split-ring resonators and their applications," *Electron. and Commun. in Japan*, pt. 2, vol. 76, no. 5, pp. 45–55, May 1993.
[15] M. Makimoto, "Microstripline split-ring resonators and their application to bandpass filters," *Electron. and Commun. in Japan*, pt. 2, vol. 12, no. 5, pp. 104–112, May 1989.
[16] M. Sagawa, K. Takahashi, and M. Makimoto, "Miniaturized hairpin resonator filters and their application to receiver front-end MIC's," *IEEE Trans. Microwave Theory Tech.*, vol. 37, pp. 1991–1997, Dec. 1989.
[17] H. Yabuki, M. Sagawa, and M. Makimoto, "An experimental study on frequency synthesizers using push-push oscillators," *IEICE Trans.*, vol. E76-J-C, no. 6, pp. 932–937, June 1993.
[18] H. Moschuring and I. Wolff, "Inhomogeneous open-ended resonators as microwave sensor elements," in *1984 IEEE MTT-S Int. Microwave Symp. Dig.*, San Francisco, CA, May 1984, pp. 187–189.
[19] M. Sagawa, H. Shirai, and M. Makimoto, "Bandpass filters using microstrip linear tapered transmission lines resonators," *IEICE Trans.*, vol. E76-C, no. 6, pp. 985–992, June 1993.
[20] V. K. Tripathi, "Asymmetric coupled transmission lines in an inhomogeneous medium," *IEEE Trans. Microwave Theory Tech.*, vol. MTT-23, pp. 734–739, Sept. 1975.
[21] S. Kanba, K. Kawabata, H. Yamada, and H. Takagi, "Dielectric constant gradient substrates," *Denshi Tokyo*, no. 33. pp. 49–52, 1994.
[22] U. Karacaoglu, I. D. Robertson, and M. Guglielmi, "An improved dual-mode microstrip ring resonator filter with simple geometry," in *Proc. 1994 European Microwave Conf.*, Cannes, France, Sept. 1994, pp. 472–477.
[23] C.-H. Ho, L. Fan, and K. Chang, "Slotline annular ring element and their applications to resonators, filters and coupler design," *IEEE Trans. Microwave Theory Tech.*, vol. 41, pp. 1648–1650, Sept. 1993.

Morikazu Sagawa (M'92) was born on May 13, 1949, in Tokyo, Japan. He received the B.S. degree in electronic engineering from the University of Electro-Communications, Tokyo, Japan, in 1973.

In 1973, he joined Matsushita Research Institute Tokyo, Inc., Tama-ku Kawasaki, Japan, where he did research and development work on microwave components—in particular, filters and oscillators. He is presently concerned with radio frequency and microwave to millimeter-wave integrated circuits. He is also engaged in research and development of radio equipment for advanced mobile communications.

Mr. Sagawa is a member of the Institute of Electronics, Information, and Communication Engineers of Japan (IEICE).

Mitsuo Makimoto (M'88) was born on September 19, 1944, in Kagoshima, Japan. He received the B.S. and M.S. degrees in electrical engineering from Yokohama National University, Yokahama, Japan, in 1968 and 1970, respectively. He received the Dr.Eng. degree from Tokyo Institute of Technology, Tokyo, Japan, in 1990.

In 1970, he joined Matsushita Research Institute Tokyo, Inc., Tama-ku Kawasaki, Japan, where he did research and development work on microwave-integrated circuits and components for radio communication systems. His current research interests include microwave devices and subsystems for advanced mobile communications.

Dr. Makimoto is a member of the Institute of Electronics, Information, and Communication Engineers of Japan (IEICE) and the Institute of Image Information and Television Engineers of Japan (ITE).

Sadahiko Yamashita (M'77) was born on March 18, 1940, in Sendai, Japan. He received the B.S. and Dr.Eng. degrees in electronic engineering from Tohoku University, Sendai, Japan, in 1962 and 1986, respectively.

In 1962, he joined Matsushita Research Institute Tokyo, Inc., Tama-ku Kawasaki, Japan, where he did research and development work on microwave-integrated circuits and components for radio communication systems. He is presently interested in microwave devices and subsystems for advanced mobile communications.

Dr. Yamashita is a member of the Institute of Electronics, Information, and Communication Engineers of Japan (IEICE) and the Institute of Image Information and Television Engineers of Japan (ITE).